Nanoscale Research Letters
a SpringerOpen Journal

NANO EXPRESS Open Access

Chitosan-based intelligent theragnosis nanocomposites enable pH-sensitive drug release with MR-guided imaging for cancer therapy

Eun-Kyung Lim[1,2†], Warayuth Sajomsang[3,4†], Yuna Choi[1], Eunji Jang[5], Hwunjae Lee[1], Byunghoon Kang[5], Eunjung Kim[5], Seungjoo Haam[2,5], Jin-Suck Suh[1,2], Sang Jeon Chung[4,6*] and Yong-Min Huh[1,2*]

Abstract

Smart drug delivery systems that are triggered by environmental conditions have been developed to enhance cancer therapeutic efficacy while limiting unwanted effects. Because cancer exhibits abnormally high local acidities compared to normal tissues (pH 7.4) due to Warburg effects, pH-sensitive systems have been researched for effective cancer therapy. Chitosan-based intelligent theragnosis nanocomposites, *N*-naphthyl-*O*-dimethymaleoyl chitosan-based drug-loaded magnetic nanoparticles (*N*Chitosan-DMNPs), were developed in this study. *N*Chitosan-DMNPs are capable of pH-sensitive drug release with MR-guided images because doxorubicin (DOX) and magnetic nanocrystals (MNCs) are encapsulated into the designed *N*-naphthyl-*O*-dimethymaleoyl chitosan (*N*-nap-*O*-MalCS). This system exhibits rapid DOX release as acidity increases, high stability under high pH conditions, and sufficient capacity for diagnosing and monitoring therapeutic responses. These results demonstrate that *N*Chitosan-DMNPs have potential as theragnosis nanocomposites for effective cancer therapy.

Keywords: Theragnosis; Cancer therapy; Drug delivery; pH-sensitive; Magnetic resonance imaging; Nanocomposites

Background

Many therapeutic anticancer drugs are limited in their clinical applications because of their toxicities and low solubility in aqueous media [1-14]. For instance, doxorubicin (DOX) is one of the most widely used drugs in cancer therapy. However, it can cause side effects such as cardiotoxicity and drug resistance. Also, it is difficult to administer intravenously because of its low solubility in aqueous media. Nanomaterial-based drug delivery systems have received attention in overcoming this drawback. These systems can be made from a variety of organic and inorganic materials including non-degradable and biodegradable polymers, and inorganic nanocrystals. Polymeric micelles based on amphiphilic block copolymers have the advantages of high biocompatibility and drug-loading capacity with low toxicity because they can self-assemble into polymeric micelles in aqueous media [8,15-17]. They accumulate in tumors through an enhanced permeation and retention (EPR) effect compared to single small molecules, leading to preferential spatio-distribution in the tumor. However, the drug release behavior of polymeric micelles is difficult to control; they freely release the drug before reaching tumors, which could give rise to unwanted side effects and low therapeutic efficacy [4,8]. Well-designed drug delivery systems need to be developed to enable cancer chemotherapy that fundamentally enhances therapeutic efficacy by minimizing drug release in undesirable sites. With these systems, a precise drug concentration can be delivered to tumors to reduce side effects. Drug delivery systems can be designed to release drugs triggered by environmental parameters such as pH, enzymes, and temperature [16,18-29]. The pH-sensitive systems are of special interest because tumors and intracellular endosomal/lysomal compartments exhibit abnormally high local acidities compared to healthy tissues with a normal physiological pH of 7.4 [9,21,25,28-43].

In this study, chitosan-based intelligent theragnosis nanocomposites that enable pH-sensitive drug release

* Correspondence: sjchung@dongguk.edu; ymhuh@yuhs.ac
†Equal contributors
[4]BioNanotechnology Research Center, KRIBB, Yuseong, Daejeon 305-806, Republic of Korea
[1]Department of Radiology, College of Medicine, Yonsei University, Seoul 120-752, South Korea
Full list of author information is available at the end of the article

with magnetic resonance (MR)-guided images were developed (Figure 1). This nanocomposite was based on *N*-naphthyl-*O*-dimethymaleoyl chitosan (*N*-nap-*O*-MalCS), a newly synthesized, pH-sensitive amphiphilic copolymer modified by maleoyl groups on a chitosan backbone. Chitosan is non-toxic, biodegradable, and non-immunogenic [44-72]. It is a linear polysaccharide consisting of *N*-acetyl-glucosamine (acetylated) and glucosamine (deacetylated) repeating units, and its abundant reactive groups facilitate chemical modification of functional groups. Hydrophobic magnetic nanocrystals were loaded as imaging agents in this system, leading to the formulation of theragnosis nanocomposites capable of delivery therapy concomitant with monitoring. This nanocomposite will allow effective cancer therapy because it can provide patient-specific drug administration strategies that consider drug-release patterns and biodistribution.

Methods

Materials

Chitosan with an average molecular weight (mol. wt.) of 15 kDa was purchased from Seafresh Industry Public Co., Ltd. (Bangkok, Thailand). The degree of chitosan deacetylation (DDA) was determined by ^{1}H-NMR spectroscopy to be 98%. Cellulose microcrystalline power, chitosan with low molecular weight, 2-naphthaldehyde, 2,3-dimethylmaleic anhydride, sodium borohydride, sodium hydroxide (NaOH), triethylamine, *N*,*N*-dimethylformamide (DMF), dimethylsulfoxide (DMSO), *N*-hydroxysulfosuccinicimide (NHS), iron(III) acetylacetonate, manganese(II) acetylacetonate, 1,2-hexadecanediol, dodecanoic acid, dodecylamine, benzyl ether, paraformaldehyde, triethylamine, 2,3-dimethylmaleic anhydride, and DOX were purchased from Sigma-Aldrich (St. Louis, MO, USA). Ethanol and chloroform (CF) were obtained from Duksan Pure Chemicals Co. (Seonggok-dong, Danwon-gu, South Korea). Dialysis tubing with a molecular weight cutoff of 3,500 g/mol was purchased from Cellu Sep T4, Membrane Filtration Products, Inc. (Segiun, TX, USA). Phosphate buffered saline (PBS; 10 mM, pH 7.4) and Dulbecco's modified eagle medium (DMEM) were purchased from Gibco (Life Technologies Corp., Carlsbad, CA, USA). All other chemicals and reagents were of analytical grade.

Synthesis of *N*-naphthyl-*O*-dimethylmaleoyl chitosan

N-naphthyl chitosan (*N*-NapCS) was synthesized by reductive amination (Figure 2a) [68]. Briefly, 1.00 g of chitosan (6.17 meq/GlcN) was dissolved in 50 mL of 1% (*v*/*v*) acetic acid (pH 4). 2-Naphthaldehyde (1.31 mL, 2.0 meq/*N*-NapCS) dissolved in 30 mL of DMF was then added and stirred at room temperature for 24 h. Solution pH was adjusted to 5 with 15% (*w*/*v*) NaOH. Subsequently, 3.50 g of sodium borohydride (15 meq/*N*-NapCS) was added and stirred at room temperature for

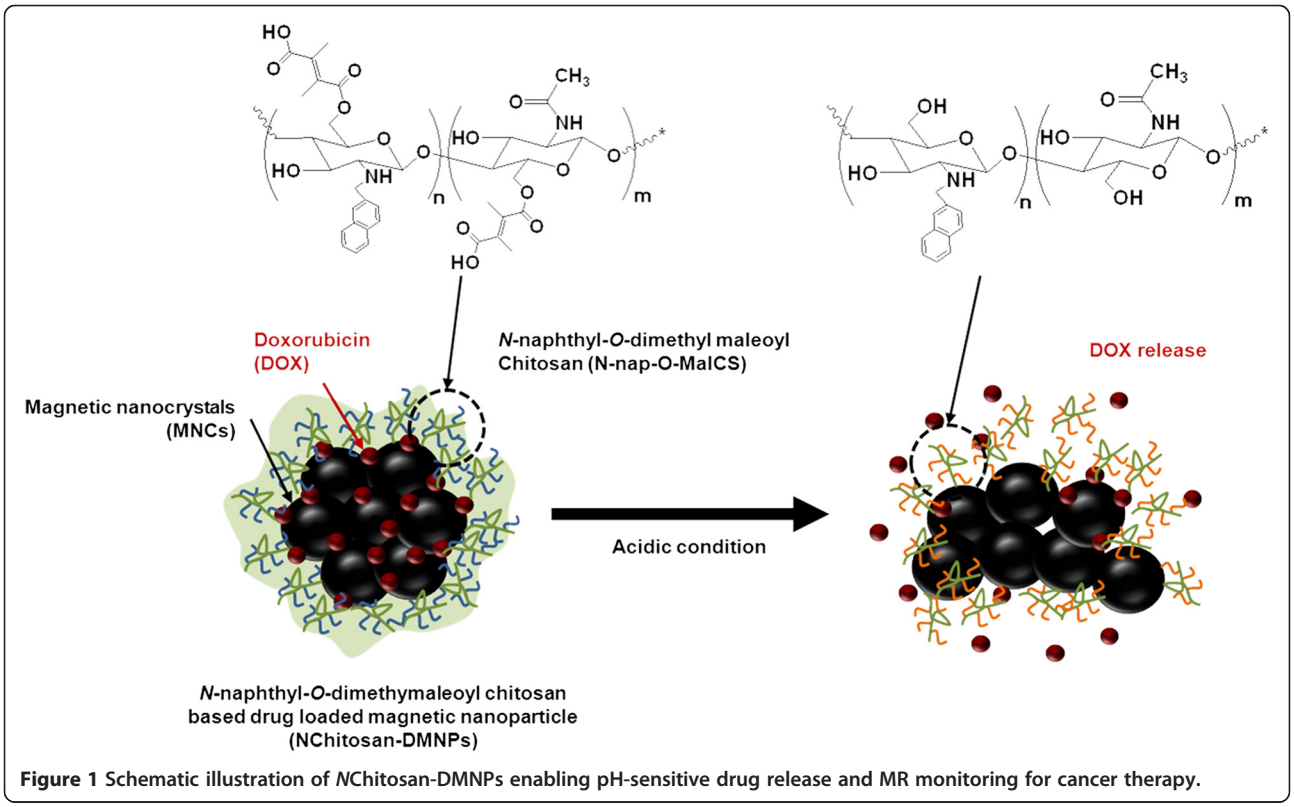

Figure 1 Schematic illustration of *N*Chitosan-DMNPs enabling pH-sensitive drug release and MR monitoring for cancer therapy.

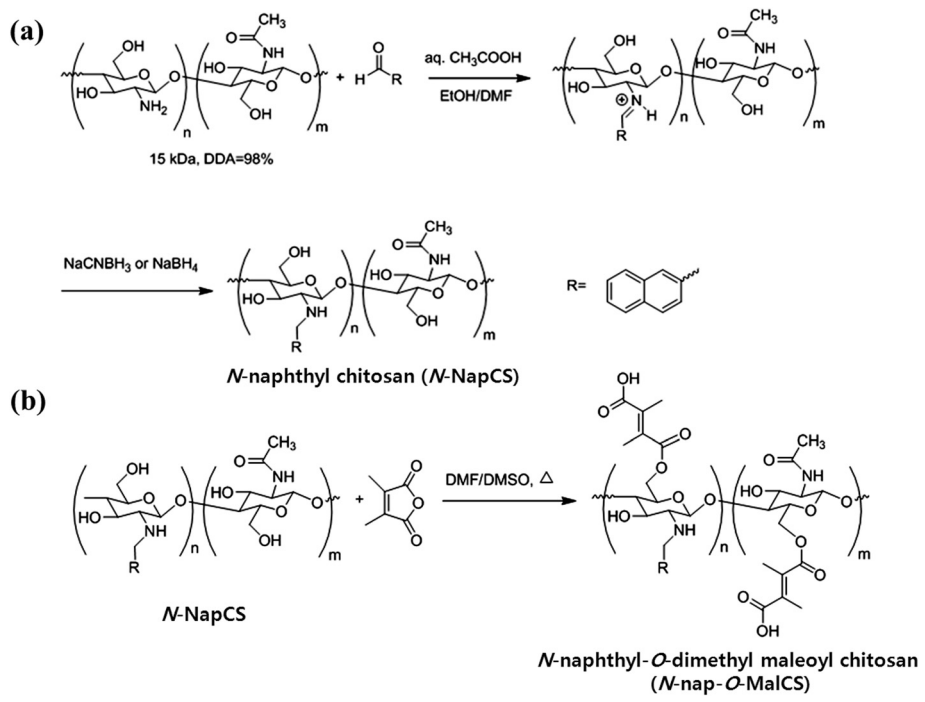

Figure 2 Synthesis of (a) *N*-NapCS and (b) *N*-naphthyl-*O*-dimethylmaleoyl chitosan (*N*-nap-*O*-MalCS).

24 h, followed by pH adjustment to 7 with 15% (*w*/*v*) NaOH. The precipitate was collected by filtration and re-dispersed in ethanol several times to remove excess aldehyde. The precipitate was then filtered, washed with ethanol, and dried under vacuum. White *N*-NapCS powder was obtained (1.78 g). Each *N*-NapCS (0.50 g) was dispersed in 30 mL of DMF/DMSO (1:1 *v*/*v*). Triethylamine with the amount of 1 mL and 1.50 g of 2,3-dimethylmaleic anhydride were added. The reaction was performed at 100°C under argon purge for 24 h (Figure 2b). The reaction mixture was cooled to room temperature and filtered to remove insoluble residue. The mixture was dialyzed with distilled water for 3 days to remove excess 2,3-dimethylmaleic anhydride and solvent. It was then freeze-dried at −85°C under vacuum conditions for 24 h. A brown *N*-nap-*O*-MalCS powder was obtained (0.58 g).

Preparation of nanopolymeric micelles

N-Nap-*O*-MalCS (12 mg) was dissolved in 12 mL of DMSO. The solution was stirred at room temperature until completely dissolved. It was then placed into a dialysis bag and dialyzed against deionized water overnight. The solution was then filtered through syringe filter membranes (cellulose acetate) with pore sizes of 0.45 μm for further study. Using the same procedure described above, the solution was then placed into a dialysis bag and dialyzed against deionized water by adjusting to pH of 8 to 9 with 5% (*w*/*v*) sodium hydroxide overnight.

Effect of pH and temperature on nanopolymeric micelles

Three milliliters of nanopolymeric micelles was placed into a dialysis bag and dialyzed against 12 mL of PBS buffer of pH 5.5, 6.0, 6.5, 6.8, 7.2, 7.4, and 8.0 at 25 and 37°C for 24 h. PBS buffer was refreshed twice. The particle sizes of nanopolymeric micelles with different pH values were analyzed in triplicate by laser scattering.

Preparation of magnetic nanocrystals

Monodispersed magnetic nanocrystals that are soluble in non-polar organic solvents were synthesized by thermal decomposition, as previously described [73-78]. Briefly, iron(III) acetylacetonate (2 mmol), manganese(II) acetylacetonate (1 mmol), 1,2-hexadecanediol (10 mmol), dodecanoic acid (6 mmol), and dodecylamine (6 mmol) were dissolved in benzyl ether (20 mL) under an ambient nitrogen atmosphere. The mixture was then preheated to 200°C for 2 h and refluxed at 300°C for 30 min. After reactants cooled down at room temperature, the products were purified with excess pure ethanol. Approximately 12 nm of magnetic nanocrystals (MNCs) were synthesized by seed-mediated growth method.

Preparation of N-naphthyl-O-dimethymaleoyl chitosan-based drug-loaded magnetic nanoparticles

N-naphthyl-*O*-dimethymaleoyl chitosan-based drug-loaded magnetic nanoparticles (*N*Chitosan-DMNPs) were fabricated by nanoemulsion methods. Fifty milligrams of MNCs and 2 mg DOX were dissolved in 4 mL

chloroform (CF). This mixture was then poured into 50 mL of pH 9.8 solution containing *N*-nap-*O*-MalCS (40 mg). The solution was ultrasonicated for 30 min and stirred overnight at room temperature to evaporate the CF. The resulting suspension was centrifuged three times for 15 min at 13,000 rpm. After the supernatant was removed, the precipitated *N*Chitosan-DMNPs were re-dispersed in 5 mL of deionized water. The size distribution and zeta potential of *N*Chitosan-DMNPs were analyzed by laser scattering (ELS-Z; Otsuka Electronics, Hirakata, Osaka, Japan). The loading ratio (%) and crystallinities of MNCs at 25°C were determined by thermogravimetric analysis (SDT-Q600, TA Instruments, New Castle, DE, USA) and X-ray diffraction (X-ray diffractometer Ultima3; Rigaku Corporation, Tokyo, Japan), respectively. The magnetic properties of *N*Chitosan-DMNPs were also analyzed using vibration sample magnetometer (VSM) (model 7407, Lake Shore Cryotonics Inc, Westerville, Columbus, OH, USA) at 25°C. The surface compositions were measured using X-ray photoelectron spectrometry (ESCALAB 250 XPS spectrometer; Thermo Fisher Scientific, Hudson, NH, USA).

Determination of drug release profile

One milliliter of the above *N*Chitosan-DMNPs was centrifuged for 45 min at 20,000 rpm, and the precipitated *N*Chitosan-DMNPs were re-dispersed in 1 mL of buffer solutions at pH 5.5, 7.4, and 9.8. The dispersed particles were sealed in dialysis tubing and immersed in 10 mL of each buffer solution at 37.5°C, which was conducted in triplicate. The amount of released drug was measured at 593 nm by fluorescence spectrometry. These results are shown as average ± standard deviation ($n = 3$). In addition, the drug loading efficiency (7.2 wt.%) was measured in the same manner. Briefly, *N*Chitosan-DMNPs' weight was measured after lyophilization and then dissolved in 1 mL of DMSO. The loaded amount of drug was measured by fluorescence spectrometry, using the following formula:

$$\begin{aligned}&\text{Drug loading effiency}\,(\text{wt.}\%)\\&\quad=(\text{Weight of drug in } N\text{Chitosan-DMNPs})/\\&\qquad(\text{Weight of } N\text{Chitosan-DMNPs})\times 100\end{aligned}$$

Cellular internalization of NChitosan-DMNPs

MR imaging and fluorescence microscopy confirmed cellular internalization of *N*Chitosan-DMNPs. NIH3T6.7 cells were obtained from American Type Culture Collection. First, these cells were seeded at a density of 1.0×10^6 cells/well in six wells for growth overnight at 37°C and then further incubated with *N*Chitosan-DMNPs in 5% CO_2 for 24 h at 37°C. The cells were washed three times with PBS and stained by Hoechst (Molecular Probes TM, OR, USA) to show nucleus location. Fluorescence microscopic images were obtained using a laser scanning confocal microscope (LSM700, Carl Zeiss, Jena, Germany). Under the same conditions, NIH3T6.7 cells treated with *N*Chitosan-DMNPs were washed twice, collected, and then re-suspended in 0.2 mL of 4% paraformaldehyde for MR imaging analysis. All experiments were conducted in triplicate.

Determination of cell viability using MTT assay

The cell viability of *N*Chitosan-DMNPs was evaluated by measuring cell growth inhibition using a 3-(4,5-dimethylthiazol-2-yl)-2,5-diphenyltetrazolium bromide (MTT) assay (Roche Molecular Biochemicals, Mannheim, Germany) compared to DOX as a control. NIH3T6.7 cells (1.0×10^4 cells/well) were implanted in a 96-microwell plate with temperature at 37°C overnight and treated with various concentrations of *N*Chitosan-DMNPs. After 24 h, the cells were washed and incubated for an additional 48 h. The yellow tetrazolium salt of MTT solution was reduced to purple formazan crystals in metabolically active cells. The cell viability was determined from the ratio of treated cells to non-treated control cells. The results are shown as average ± standard deviation ($n = 4$).

Animal experiments

All animal experiments were conducted with approval from the Association for Assessment and Accreditation of Laboratory Animal Care (AAALAC) International. Tumor-bearing mice were developed, and NIH3T6.7 cells (5×10^6 cells suspended in 50 μL saline per animal) were implanted into the proximal thighs of female BALB/nude mice (4 to 5 weeks of age) to investigate *N*Chitosan-DMNPs' distribution and tumor growth rate. After tumor volume reached approximately 40 mm^3 at 3 days post-implantation (0 days), *in vivo* magnetic resonance imaging (MRI) experiments were performed using *N*Chitosan-DMNPs (five mice). Comparative therapeutic efficacy was evaluated using three groups (saline, doxorubicin, and *N*Chitosan-DMNP) of mice (ten mice per each group). Animals were treated with equivalent doses of DOX (3 mg/kg) and *N*Chitosan-DMNPs suspended in PBS by intravenous injection every 2 days for 12 days. At predetermined time periods, the length of the minor axis (2a) and major axis (2b) of each tumor was measured using a caliper. Each tumor volume was then calculated using the formula for ellipsoid $[(4/3)\pi \times a^2 b]$.

MR imaging

In vivo MR imaging experiments were performed using a 3.0 T clinical MRI instrument with a micro-47 surface coil (Intera; Philips Medical Systems, Best, The Netherlands).

The *T*2 weights of nude mice injected with nanoparticles were measured by Carr-Purcell-Meiboom-Gill sequence at room temperature with the following parameters: TR = 10 s, echoes = 32 with 12 ms even echo space, number of acquisitions = 1, point resolution = 156 × 156 μm, and section thickness = 0.6 mm. For *T*2-weighted MR imaging in the nude mouse model, the following parameters were adopted: resolution = 234 × 234 μm^2, section thickness = 2.0 mm, TE = 60 ms, TR = 4,000 ms, and number of acquisitions = 1.

Results and discussion

Characterization of *N*-naphthyl-*O*-dimethymaleoyl chitosan

N-naphthyl-*O*-dimethymaleoyl chitosan was synthesized by modifying chitosan with naphthyl groups at amino groups to complement their solubility and introduce amphiphilic properties [79]. Chitosan was reacted with naphthaldehyde to obtain an imine (Schiff base), which is easily converted into an *N*-naphthyl derivate by reduction with sodium borohydride or sodium cyanoborohydride (Figure 2a). Afterward, *N*-NapCS was introduced into the hydroxyl groups of chitosan by maleoylation with dimethylmaleic anhydride in DMF/DMSO to obtain *N*-nap-*O*-MalCS (Figure 2b) [67,68]. This synthetic compound was characterized by a ^{1}H-NMR spectrum, and satisfactory analysis data were obtained (Figure 3). *N*-nap-*O*-MalCS was used to form nanopolymeric micelles by dialysis in various pH solutions. They were less than 200 nm at pH 7.2 to 8.0 but rapidly increased in size as the acidity of solution increased (Figure 4). Their sizes could not be measured at pH 5.5 and 6.0 (Figure 4a) due to aggregation. This was a result of the weakened solubility of *N*-nap-*O*-MalCS in the aqueous phase caused by acid hydrolysis of its maleoyl groups [80,81]. This phenomenon accelerated at 37°C compared to 25°C (Figure 4b). *N*-Nap-*O*-MalCS has a potential as a drug carrier because it can self-assemble with pH-sensitive behavior [67,68,79,82].

Characterization of *N*-naphthyl-*O*-dimethymaleoyl chitosan-based drug-loaded magnetic nanoparticles

NChitosan-DMNPs were prepared by a nanoemulsion method, in which naphtyl groups were absorbed on the hydrophobic surface of MNCs and DOX mainly caused by *van der Waals* force, and both their oxygen atoms and water molecules were interacted by hydrogen bonding. This interaction could lead to formation of *N*Chitosan-DMNPs dispersed in aqueous phase with high colloidal stability. *N*Chitosan-DMNPs were loaded with 27.5 wt.% MNCs and exhibited superparamagnetic behavior with a magnetization saturation value of 40.4 emu/$g_{Fe + Mn}$ at 1.2 T (Figure 5). In addition, iron (Fe) and manganese (Mn) were not detected by X-ray photoelectron spectroscopy (XPS) analysis, which indicates that MNCs were safely encapsulated inside the *N*Chitosan-DMNPs (Figure 5). The availability of *N*Chitosan-DMNPs as MRI contrast agents was evaluated by measuring spin-spin relaxation times (*T*2) of water protons in the aqueous

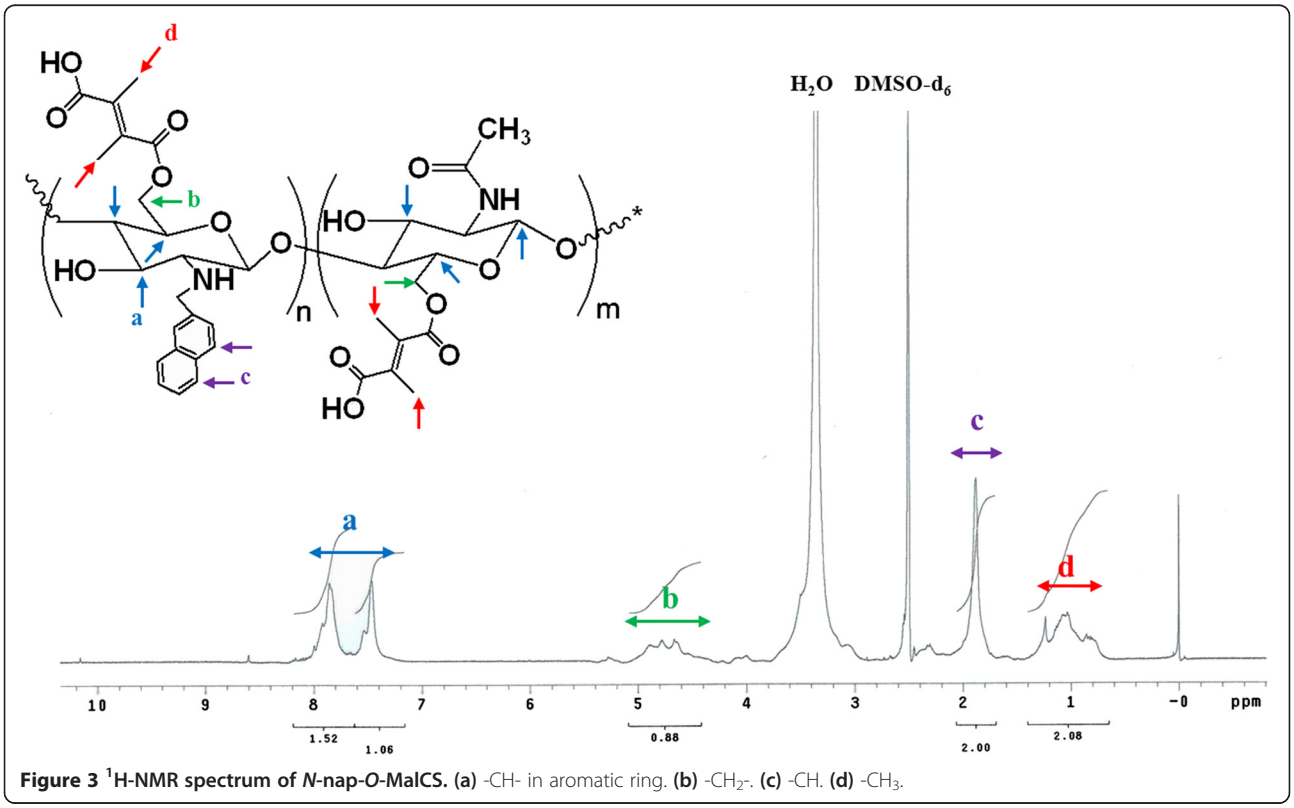

Figure 3 ^{1}**H-NMR spectrum of *N*-nap-*O*-MalCS. (a)** -CH- in aromatic ring. **(b)** $-CH_2-$. **(c)** -CH. **(d)** $-CH_3$.

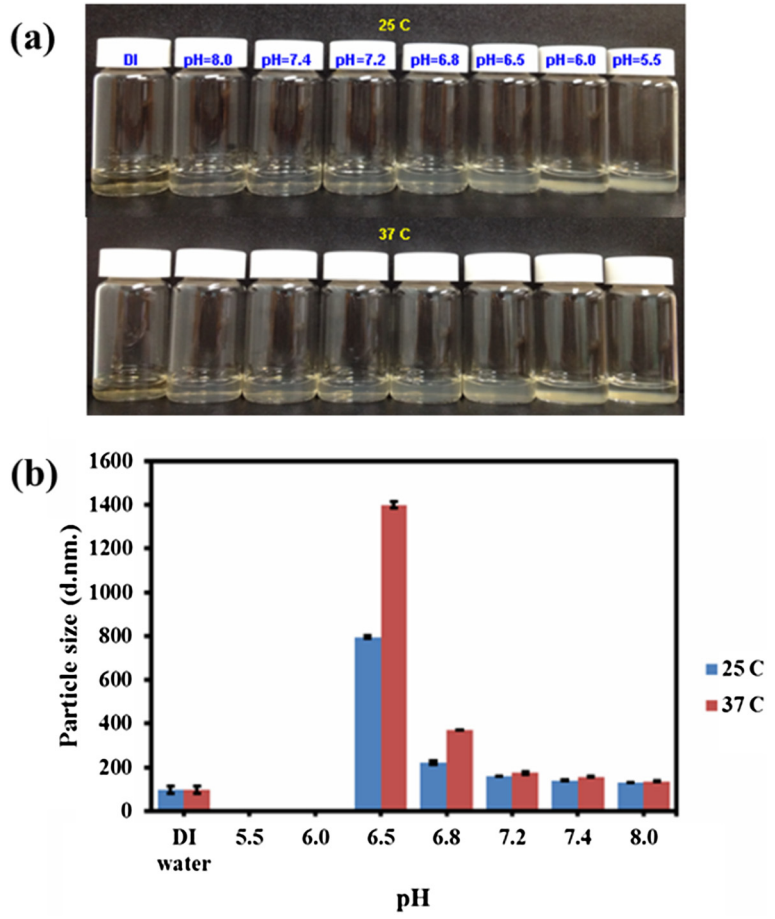

Figure 4 Effect of *N*-nap-*O*-MalCS polymeric micelles in various pH conditions and temperatures. (a) Stability. **(b)** Particle size.

solutions using 1.5-T MR images. As the concentration of MNCs (Fe + Mn) in *N*Chitosan-DMNPs increased, the MR image was proportionally darkened with an *R*2 coefficient of 254.6/mMs, demonstrating that *N*Chitosan-DMNPs have sufficient ability as MRI contrast agents (Figure 6).

pH-sensitive drug release properties

To investigate the pH-dependent behavior of *N*Chitosan-DMNPs, they were dispersed in different pH solutions (pH 5.5, 7.4, and 9.8) and their sizes were analyzed using laser scattering. *N*Chitosan-DMNPs in a pH 9.8 solution showed stable particle size around 100 nm (100.3 ± 4.9 nm), but their sizes increased slightly with increased buffer solution acidity (pH 5.5, 185.3 ± 13.5 nm and pH 7.4, 158.8 ± 10.6 nm) (Figure 7a) [17,20,30,83,84]. This is because the solubility of *N*-nap-*O*-MalCS of *N*Chitosan-DMNPs was weakened by acid hydrolysis of maleoyl groups, as mentioned above. This pH-dependent behavior was expected to induce pH-sensitive drug release profiles. DOX was abruptly released from *N*Chitosan-DMNPs under acidic conditions (pH 5.5) with about 90% of drug release within 24 h (Figure 7b), whereas only 20% of DOX was released at higher pH conditions (pH 7.4 and 9.8) during the same time period and both release profiles showed sustained release patterns for 8 days. This result implies that drugs could be released more from *N*Chitosan-DMNPs in acidic tumor sites than in normal tissues with decreased drug loss during blood circulation. After *N*Chitosan-DMNPs internalization by endocytosis, drug release could be further accelerated inside the acidic endosomes of tumor cells.

Cellular uptake and cytotoxicity

NIH3T6.7 cells were treated with *N*Chitosan-DMNPs and observed by confocal laser fluorescence microscopy to confirm their cellular uptake. Blue fluorescence indicated cell nuclei by Hoechst stains and red fluorescent signals are derived from cell nuclei and DOX. In Figure 8a, red fluorescence was generally observed in the intracellular regions, indicating released DOX from internalized *N*Chitosan-DMNPs. NIH3T6.7 cells incubated with *N*Chitosan-DMNPs also showed MR contrast effects compared to

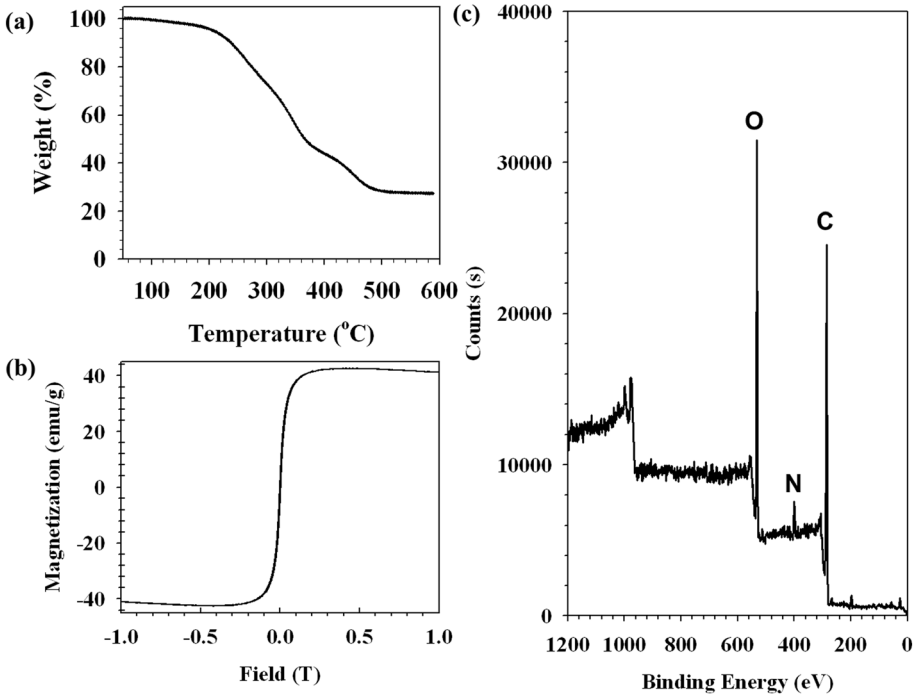

Figure 5 Characterizations of *N*Chitosan-DMNPs. (a) Thermogravimetric analysis (TGA), **(b)** magnetic hysteresis loops, and **(c)** XPS patterns of *N*-naphtyl-*O*-dimethymaleoyl chitosan-based drug-loaded magnetic nanoparticles (*N*Chitosan-DMNPs).

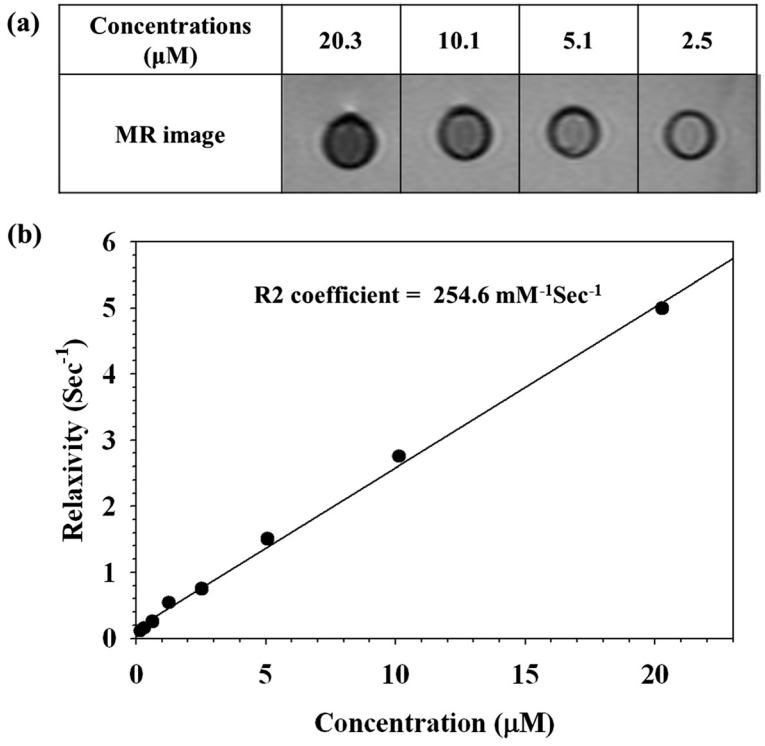

Figure 6 Assessment of the ability of *N*Chitosan-DMNPs as MRI contrast agents. (a) *T*2-weighted MR images of *N*Chitosan-DMNPs in aqueous solution and **(b)** relaxation rate (*R*2) versus *N*Chitosan-DMNPs concentration.

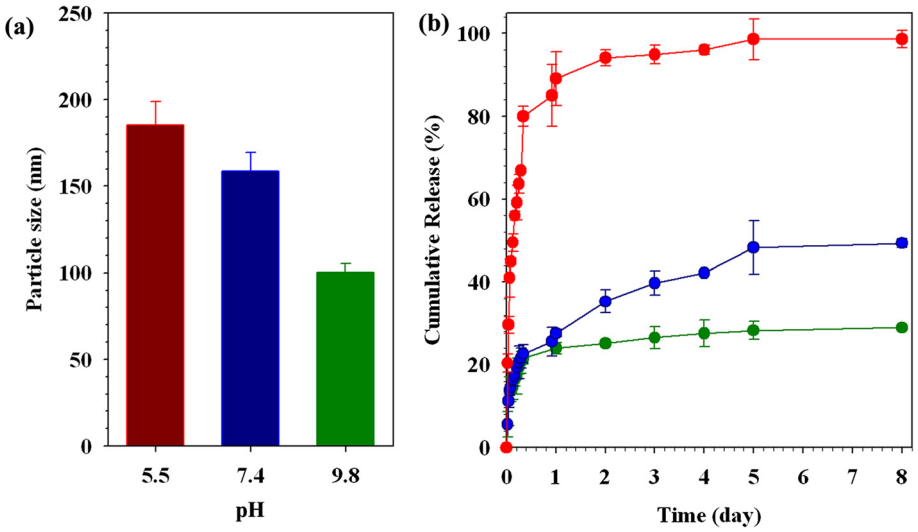

Figure 7 Particle size of *N*Chitosan-DMNPs in different pH conditions (a) and pH-sensitive drug release profiles (b). Red pH 5.5, blue pH 7.4, and green pH 9.8.

non-treated cells (non-treatment) (Figure 8b). The MR signal of NIH3T6.7 cells treated with *N*Chitosan-DMNPs was about 1.72-fold higher than that of non-treated cells, with an *R*2 value of 22.1/s (*R*2 value of non-treated cells: 8.10/s). The cytotoxicity of *N*Chitosan-DMNPs against NIH3T6.7 cells was evaluated by MTT assay (Figure 9) [85-87]. DOX-treated cells were also evaluated under the same conditions as a control.

DOX and *N*Chitosan-DMNPs exhibited dose-dependent cytotoxic effects on NIH3T6.7. DOX showed a higher cytotoxicity than *N*Chitosan-DMNPs because *N*Chitosan-DMNPs released DOX after their cellular internalization, while free DOX directly diffused and penetrated through cell membranes due to its low molecular weight.

In vivo *theranostic effects of* N*Chitosan-DMNPs*

The theranostic effects of *N*Chitosan-DMNPs were confirmed against an *in vivo* model [9,88,89]. To determine the therapeutic dosing schedule, intratumoral distributions

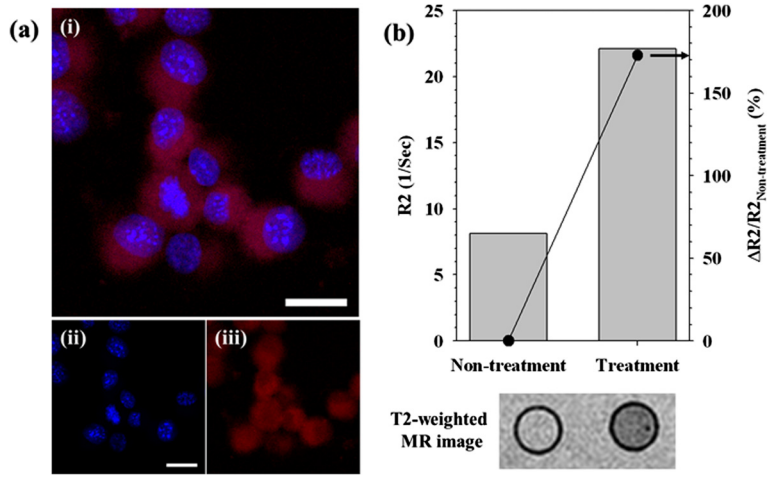

Figure 8 Cellular internalization efficacy of *N*Chitosan-DMNPs. (a) Fluorescence image of *N*Chitosan-DMNP-treated cells (i, merged image; ii, blue filter for Hoechst; iii, red filter for DOX). **(b)** *T*2-weighted MR image and graph of $\Delta R2/R2$ non-treatment for *N*Chitosan-DMNP-treated cells. Scale bars 50 μm.

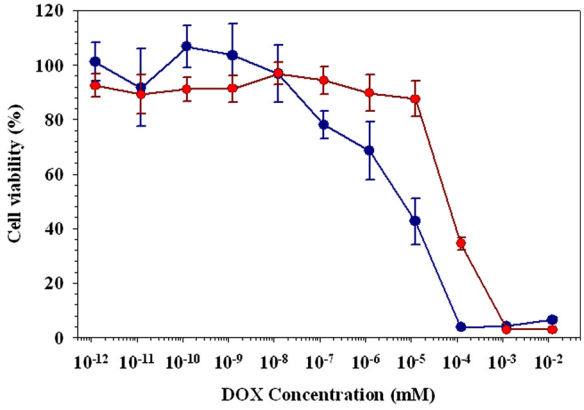

Figure 9 Cell viability test of cells treated with DOX and *N*Chitosan-DMNPs (red, *N*Chitosan-DMNPs; blue, DOX).

of *N*Chitosan-DMNPs in tumor-bearing mice were investigated through MR images after intravenous injection into mouse tail veins (150 μg Fe + Mn, 3 mg/kg DOX). After injecting *N*Chitosan-DMNPs (post-injection), the black color gradually spread out in *T*2-weighted MR images following the peripheral blood vessels of the tumor area. This resulted from diffusion and permeation to tumor tissues across corresponding vascular distributions by an EPR effect (Figure 10a). The therapeutic dosing of *N*Chitosan-DMNPs were determined because these were maximally delivered within 1 h at the tumor sites and then over 80% of drug was released in the in the acidic environments within the tumor for 24 h, as judged from *in vivo* MRI and drug release profiling studies. Considering these results, we determined 2 days periodically to consistently maintain drug concentration within tumors for effective cancer therapy. NChitosan-DMNPs, free DOX, and saline were administrated to each subgroup of tumor-bearing mice via intravenous (i.v.) injection every 2 days for 12 days (injection on days 0, 2, 4, 6, 8, 10, and 12). Tumor sizes were monitored for 24 days. *N*Chitosan-DMNPs exhibited significant tumor growth inhibition with an average tumor growth rate of 1,638.1 ± 306.9% compared to the control (free DOX and saline) groups (saline, 4,642.8%; free DOX, 2,991.9%) (Figure 10b). Although *N*Chitosan-DMNPs could not completely suppress tumor growth, tumor growth inhibition was more effective than with saline or free DOX. During the experimental period, no loss in mice body weight was observed.

Conclusions

We have formulated theranostic nanocomposites, *N*Chitosan-DMNPs, based on *N*-nap-*O*-MalCS for effective cancer therapy. *N*Chitosan-DMNPs exhibited a pH-sensitive drug release pattern with MR imaging due to the pH-sensitive properties of *N*-nap-*O*-MalCS. Furthermore, theragnostic efficacies of *N*Chitosan-DMNPs were confirmed in the *in vivo* model by determining their therapeutic dosing schedule based on drug release profiling and *in vivo* MRI study. From these results, *N*Chitosan-DMNPs are expected to play a significant role in the dawning era of personalized medicine.

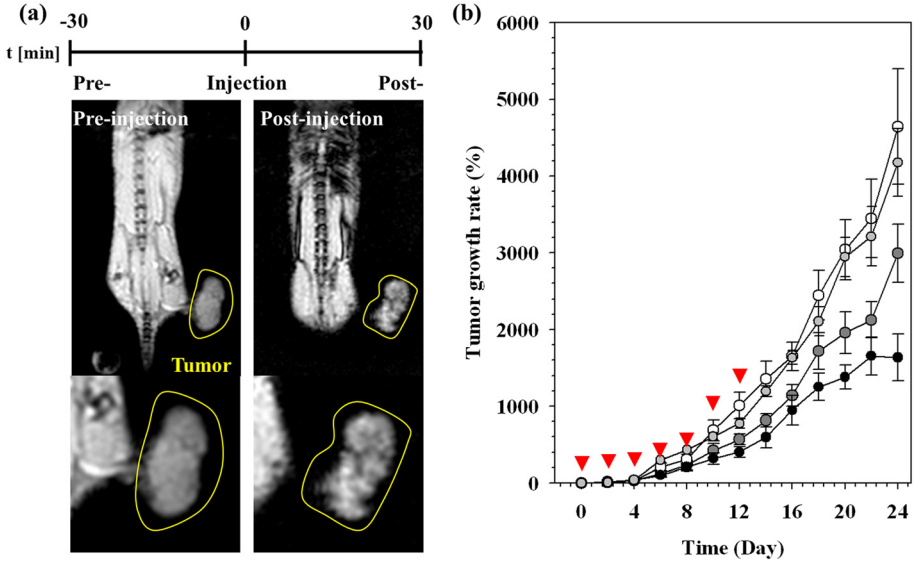

Figure 10 MR imaging to assess intratumoral distributions of *N*Chitosan-DMNPs in tumor-bearing mice and comparative therapeutic efficacy. **(a)** *T*2-weighted MR images of tumor-bearing mice after intravenous injection of *N*Chitosan-DMNPs. Tumor regions are indicated with a yellow line boundary. **(b)** Comparative therapeutic efficacy study in the *in vivo* model (black, *N*Chitosan-DMNPs; gray, DOX; white, saline). Red arrowheads indicate the therapeutic dosing schedule of each therapeutic condition (*N*Chitosan-DMNPs, DOX, and saline).

Abbreviations
DMNPs: Drug-loaded magnetic nanoparticles; DOX: Doxorubicin; MNCs: Magnetic nanocrystals; MRI: Magnetic resonance imaging.

Competing interests
The authors declare that they have no competing interests.

Authors' contributions
EKL and WS performed the experiments, suggested the scheme, and wrote the manuscript. YC and EJ performed the experiments. HL, BK, and EK reviewed the scheme and contents. SH and JSS revised the manuscript critically for important intellectual content. SJC and YMH supervised the project. All authors read and approved the final manuscript.

Acknowledgements
This study was supported by a grant from the National Research Foundation of Korea (NRF) funded by the Ministry of Education, Science & Technology (2012-2043991) and the Korean government (MEST) (2010-0019923). It was also supported by a grant from the KRCF Research Initiative Program and the Dongguk University Research Fund of 2013.

Author details
[1]Department of Radiology, College of Medicine, Yonsei University, Seoul 120-752, South Korea. [2]YUHS-KRIBB Medical Convergence Research Institute, Seoul 120-752, South Korea. [3]Nanodelivery System Laboratory (NDS), National Nanotechnology Center (NANOTEC), National Science and Technology Development Agency (NSTDA), Thailand Science Park, Pathumthani 12120, Thailand. [4]BioNanotechnology Research Center, KRIBB, Yuseong, Daejeon 305-806, Republic of Korea. [5]Department of Chemical and Biomolecular Engineering, Yonsei University, Seoul 120-749, South Korea. [6]Department of Chemistry, Dongguk University, Seoul 100-715, South Korea.

Received: 13 September 2013 Accepted: 27 October 2013
Published: 8 November 2013

References

1. Janib SM, Moses AS, MacKay JA: **Imaging and drug delivery using theranostic nanoparticles.** *Adv Drug Deliv Rev* 2010, **62:**1052–1063.
2. Cho H, Dong Z, Pauletti G, Zhang J, Xu H, Gu H, Wang L, Ewing R, Huth C, Wang F, Shi D: **Fluorescent, superparamagnetic nanospheres for drug storage, targeting, and imaging: a multifunctional nanocarrier system for cancer diagnosis and treatment.** *ACS Nano* 2010, **4:**5398–5404.
3. Wang J, Sun X, Mao W, Sun W, Tang J, Sui M, Shen Y, Gu Z: **Tumor redox heterogeneity-responsive prodrug nanocapsules for cancer chemotherapy.** *Adv Mater* 2013, **25:**3670–3676.
4. Secret E, Smith K, Dubljevic V, Moore E, Macardle P, Delalat B, Rogers ML, Johns TG, Durand JO, Cunin F, Voelcker NH: **Antibody-functionalized porous silicon nanoparticles for vectorization of hydrophobic drugs.** *Adv Healthc Mater* 2013, **2:**718–727.
5. Win KY, Ye E, Teng CP: *Jiang S.* Engineering polymeric microparticles as theranostic carriers for selective delivery and cancer therapy. Adv Healthc Mater: Han MY; 2013. doi:10.1002/adhm.201300077.
6. Park H, Tsutsumi H, Mihara H: **Cell penetration and cell-selective drug delivery using alpha-helix peptides conjugated with gold nanoparticles.** *Biomaterials* 2013, **34:**4872–4879.
7. Lu J, Liong M, Zink JI, Tamanoi F: **Mesoporous silica nanoparticles as a delivery system for hydrophobic anticancer drugs.** *Small* 2007, **3:**1341–1346.
8. Lim E-K, Jang E, Lee K, Haam S, Huh Y-M: **Delivery of cancer therapeutics using nanotechnology.** *Pharmaceutics* 2013, **5:**294–317.
9. Lim EK, Huh YM, Yang J, Lee K, Suh JS, Haam S: **pH-triggered drug-releasing magnetic nanoparticles for cancer therapy guided by molecular imaging by MRI.** *Adv Mater* 2011, **23:**2436–2442.
10. Liu J, Yu M, Zhou C, Yang S, Ning X, Zheng J: **Passive tumor targeting of renal-clearable luminescent gold nanoparticles: long tumor retention and fast normal tissue clearance.** *J Am Chem Soc* 2013. doi:10.1021/ja401612x.
11. Gultepe E, Nagesha D, Sridhar S, Amiji M: **Nanoporous inorganic membranes or coatings for sustained drug delivery in implantable devices.** *Adv Drug Deliv Rev* 2010, **62:**305–315.
12. Larson N, Ghandehari H: **Polymeric conjugates for drug delivery.** *Chem Mater* 2012, **24:**840–853.
13. Ganta S, Devalapally H, Shahiwala A, Amiji M: **A review of stimuli-responsive nanocarriers for drug and gene delivery.** *J Control Release* 2008, **126:**187–204.
14. Faraji AH, Wipf P: **Nanoparticles in cellular drug delivery.** *Bioorg Med Chem* 2009, **17:**2950–2962.
15. Kamada H, Tsutsumi Y, Yoshioka Y, Yamamoto Y, Kodaira H, Tsunoda S-i, Okamoto T, Mukai Y, Shibata H, Nakagaw S, Mayumi T: **Design of a pH-sensitive polymeric carrier for drug release and its application in cancer therapy.** *Clin Cancer Res* 2004, **10:**2545–2550.
16. Prabaharan M, Grailer JJ, Pilla S, Steeber DA, Gong S: **Amphiphilic multi-arm-block copolymer conjugated with doxorubicin via pH-sensitive hydrazone bond for tumor-targeted drug delivery.** *Biomaterials* 2009, **30:**5757–5766.
17. Zhang CY, Yang YQ, Huang TX, Zhao B, Guo XD, Wang JF, Zhang LJ: **Self-assembled pH-responsive MPEG-b-(PLA-co-PAE) block copolymer micelles for anticancer drug delivery.** *Biomaterials* 2012, **33:**6273–6283.
18. Kosif I, Cui M, Russell TP, Emrick T: **Triggered in situ disruption and inversion of nanoparticle-stabilized droplets.** *Angew Chem Int Ed Engl* 2013, **52:**6620–6623.
19. Zhang Y, Yin Q, Yin L, Ma L, Tang L, Cheng J: **Chain-shattering polymeric therapeutics with on-demand drug-release capability.** *Angew Chem Int Ed Engl* 2013, **52:**6435–6439.
20. Kamimura M, Kim JO, Kabanov AV, Bronich TK, Nagasaki Y: **Block ionomer complexes of PEG-block-poly(4-vinylbenzylphosphonate) and cationic surfactants as highly stable, pH responsive drug delivery system.** *J Control Release* 2012, **160:**486–494.
21. Ma L, Liu M, Shi X: **pH- and temperature-sensitive self-assembly microcapsules/microparticles: synthesis, characterization, *in vitro* cytotoxicity, and drug release properties.** *J Biomed Mater Res B Appl Biomater* 2011. doi:10.1002/jbm.b.31900.
22. Park HS, Lee JE, Cho MY, Hong JH, Cho SH, Lim YT: **Hyaluronic acid/poly (beta-amino ester) polymer nanogels for cancer-cell-specific NIR fluorescence switch.** *Macromol Rapid Commun* 2012, **33:**1549–1555.
23. Win PP, Shin-ya Y, Hong K-J, Kajiuchi T: **Formulation and characterization of pH sensitive drug carrier based on phosphorylated chitosan (PCS).** *Carbohydr Polym* 2003, **53:**305–310.
24. Lu T, Wang Z, Ma Y, Zhang Y, Chen T: **Influence of polymer size, liposomal composition, surface charge, and temperature on the permeability of pH-sensitive liposomes containing lipid-anchored poly(2-ethylacrylic acid).** *Int J Nanomedicine* 2012, **7:**4917–4926.
25. Gao GH, Park MJ, Li Y, Im GH, Kim JH, Kim HN, Lee JW, Jeon P, Bang OY, Lee JH, Lee DS: **The use of pH-sensitive positively charged polymeric micelles for protein delivery.** *Biomaterials* 2012, **33:**9157–9164.
26. Song L, Ho VH, Chen C, Yang Z, Liu D, Chen R, Zhou D: **Efficient, pH-triggered drug delivery using a pH-responsive DNA-conjugated gold nanoparticle.** *Adv Healthc Mater* 2013, **2:**275–280.
27. Tang H, Guo J, Sun Y, Chang B, Ren Q, Yang W: **Facile synthesis of pH sensitive polymer-coated mesoporous silica nanoparticles and their application in drug delivery.** *Int J Pharm* 2011, **421:**388–396.
28. Kim JK, Garripelli VK, Jeong UH, Park JS, Repka MA, Jo S: **Novel pH-sensitive polyacetal-based block copolymers for controlled drug delivery.** *Int J Pharm* 2010, **401:**79–86.
29. Du Y, Chen W, Zheng M, Meng F, Zhong Z: **pH-sensitive degradable chimaeric polymersomes for the intracellular release of doxorubicin hydrochloride.** *Biomaterials* 2012, **33:**7291–7299.
30. Xue Y, Guan Y, Zheng A, Xiao H: **Amphoteric calix[8]arene-based complex for pH-triggered drug delivery.** *Colloids Surf B: Biointerfaces* 2013, **101:**55–60.
31. Jang E, Lim E-K, Choi Y, Kim E, Kim H-O, Kim D-J, Suh J-S, Huh Y-M, Haam S: **π-Hyaluronan nanocarriers for CD44-targeted and pH-boosted aromatic drug delivery.** *J Mater Chem B* 2013, **1:**5686.
32. Lee ES, Gao Z, Kim D, Park K, Kwon IC, Bae YH: **Super pH-sensitive multifunctional polymeric micelle for tumor pH(e) specific TAT exposure and multidrug resistance.** *J Control Release* 2008, **129:**228–236.
33. Shim MS, Kwon YJ: **Stimuli-responsive polymers and nanomaterials for gene delivery and imaging applications.** *Adv Drug Deliv Rev* 2012, **64:**1046–1059.
34. Chen Z, Xu L, Liang Y, Zhao M: **pH-sensitive water-soluble nanospheric imprinted hydrogels prepared as horseradish peroxidase mimetic enzymes.** *Adv Mater* 2010, **22:**1488–1492.
35. Felber AE, Dufresne MH, Leroux JC: **pH-sensitive vesicles, polymeric micelles, and nanospheres prepared with polycarboxylates.** *Adv Drug Deliv Rev* 2012, **64:**979–992.

36. Ko JY, Park S, Lee H, Koo H, Kim MS, Choi K, Kwon IC, Jeong SY, Kim K, Lee DS: **pH-Sensitive nanoflash for tumoral acidic pH imaging in live animals.** *Small* 2010, **6:**2539–2544.
37. Koren E, Apte A, Jani A, Torchilin VP: **Multifunctional PEGylated 2C5-immunoliposomes containing pH-sensitive bonds and TAT peptide for enhanced tumor cell internalization and cytotoxicity.** *J Control Release* 2012, **160:**264–273.
38. Zhou L, Cheng R, Tao H, Ma S, Guo W, Meng F, Liu H, Liu Z, Zhong Z: **Endosomal pH-activatable poly(ethylene oxide)-graft-doxorubicin prodrugs: synthesis, drug release, and biodistribution in tumor-bearing mice.** *Biomacromolecules* 2011, **12:**1460–1467.
39. You JO, Auguste DT: **The effect of swelling and cationic character on gene transfection by pH-sensitive nanocarriers.** *Biomaterials* 2010, **31:**6859–6866.
40. Sato K, Yoshida K, Takahashi S, Anzai J: **pH- and sugar-sensitive layer-by-layer films and microcapsules for drug delivery.** *Adv Drug Deliv Rev* 2011, **63:**809–821.
41. Ryu JH, Koo H, Sun IC, Yuk SH, Choi K, Kim K, Kwon IC: **Tumor-targeting multi-functional nanoparticles for theragnosis: new paradigm for cancer therapy.** *Adv Drug Deliv Rev* 2012, **64:**1447–1458.
42. Hussain T, Nguyen QT: **Molecular imaging for cancer diagnosis and surgery.** *Adv Drug Deliv Rev* 2013. doi:10.1016/j.addr.2013.09.007.
43. Veiseh O, Kievit FM, Ellenbogen RG, Zhang M: **Cancer cell invasion: treatment and monitoring opportunities in nanomedicine.** *Adv Drug Deliv Rev* 2011, **63:**582–596.
44. Dufes C, Muller J-M, Couet W, Olivier J-C, Uchegbu IF, Schatzlein AG: **Anti-cancer drug delivery with transferrin targeted polymeric chitosan vesicles.** *Pharm Res* 2004, **21:**101–107.
45. Kim JH, Kim YS, Park K, Lee S, Nam HY, Min KH, Jo HG, Park JH, Choi K, Jeong SY, Park RW, Kim IS, Kim K, Kwon IC: **Antitumor efficacy of cisplatin-loaded glycol chitosan nanoparticles in tumor-bearing mice.** *J Control Release* 2008, **127:**41–49.
46. Nam HY, Kwon SM, Chung H, Lee SY, Kwon SH, Jeon H, Kim Y, Park JH, Kim J, Her S, Oh YK, Kwon IC, Kim K, Jeong SY: **Cellular uptake mechanism and intracellular fate of hydrophobically modified glycol chitosan nanoparticles.** *J Control Release* 2009, **135:**259–267.
47. Riva R, Ragelle H, Rieux A, Duhem N, Jérôme C, Préat V: **Chitosan and chitosan derivatives in drug delivery and tissue engineering.** *Adv Polym Sci* 2011, **244:**19–44.
48. Bhumkar DR, Joshi HM, Sastry M, Pokharkar VB: **Chitosan reduced gold nanoparticles as novel carriers for transmucosal delivery of insulin.** *Pharm Res* 2007, **24:**1415–1426.
49. Lee D, Singha K, Jang MK, Nah JW, Park IK, Kim WJ: **Chitosan: a novel platform in proton-driven DNA strand rearrangement actuation.** *Mol Biosyst* 2009, **5:**391–396.
50. Wu W, Shen J, Banerjee P, Zhou S: **Chitosan-based responsive hybrid nanogels for integration of optical pH-sensing, tumor cell imaging and controlled drug delivery.** *Biomaterials* 2010, **31:**8371–8381.
51. Ragelle H, Vandermeulen G, Preat V: **Chitosan-based siRNA delivery systems.** *J Control Release* 2013, **172:**207–218.
52. Bao H, Pan Y, Ping Y, Sahoo NG, Wu T, Li L, Li J, Gan LH: **Chitosan-functionalized graphene oxide as a nanocarrier for drug and gene delivery.** *Small* 2011, **7:**1569–1578.
53. Liu Y, Tang J, Chen X, Xin JH: **Decoration of carbon nanotubes with chitosan.** *Carbon N Y* 2005, **43:**3178–3180.
54. Dharmala K, Yoo JW, Lee CH: **Development of chitosan-SLN microparticles for chemotherapy: in vitro approach through efflux-transporter modulation.** *J Control Release* 2008, **131:**190–197.
55. Jiang HL, Kwon JT, Kim EM, Kim YK, Arote R, Jere D, Jeong HJ, Jang MK, Nah JW, Xu CX, Park IK, Cho MH, Cho CS: **Galactosylated poly(ethylene glycol)-chitosan-graft-polyethylenimine as a gene carrier for hepatocyte-targeting.** *J Control Release* 2008, **131:**150–157.
56. Bahadur KCR, Lee SM, Yoo ES, Choi JH, Ghim HD: **Glycoconjugated chitosan stabilized iron oxide nanoparticles as a multifunctional nanoprobe.** *Mater Sci Eng C* 2009, **29:**1668–1673.
57. Oh KS, Kim RS, Lee J, Kim D, Cho SH, Yuk SH: **Gold/chitosan/pluronic composite nanoparticles for drug delivery.** *J Appl Polym Sci* 2008, **108:**3239–3244.
58. Min KH, Park K, Kim YS, Bae SM, Lee S, Jo HG, Park RW, Kim IS, Jeong SY, Kim K, Kwon IC: **Hydrophobically modified glycol chitosan nanoparticles-encapsulated camptothecin enhance the drug stability and tumor targeting in cancer therapy.** *J Control Release* 2008, **127:**208–218.
59. Ta HT, Dass CR, Dunstan DE: **Injectable chitosan hydrogels for localised cancer therapy.** *J Control Release* 2008, **126:**205–216.
60. Watthanaphanit A, Supaphol P, Furuike T, Tokura S, Tamura H, Rujiravanit R: **Novel chitosan-spotted alginate fibers from wet-spinning of alginate solutions containing emulsified chitosan-citrate complex and their characterization.** *Biomacromolecules* 2009, **10:**320–327.
61. Trapani A, Garcia-Fuentes M, Alonso MJ: **Novel drug nanocarriers combining hydrophilic cyclodextrins and chitosan.** *Nanotechnology* 2008, **19:**185101.
62. Lai WF, Lin MC: **Nucleic acid delivery with chitosan and its derivatives.** *J Control Release* 2009, **134:**158–168.
63. Kievit FM, Veiseh O, Bhattarai N, Fang C, Gunn JW, Lee D, Ellenbogen RG, Olson JM, Zhang M: **PEI-PEG-chitosan copolymer coated iron oxide nanoparticles for safe gene delivery: synthesis, complexation, and transfection.** *Adv Funct Mater* 2009, **19:**2244–2251.
64. Kwon S, Park JH, Chung H, Kwon IC, Jeong SY: **Physicochemical characteristics of self-assembled nanoparticles based on glycol chitosan bearing 5-cholanic.** *Langmuir* 2003, **19:**10188–10193.
65. Cafaggi S, Russo E, Stefani R, Leardi R, Caviglioli G, Parodi B, Bignardi G, De Totero D, Aiello C, Viale M: **Preparation and evaluation of nanoparticles made of chitosan or N-trimethyl chitosan and a cisplatin-alginate complex.** *J Control Release* 2007, **121:**110–123.
66. Lee CM, Jeong HJ, Kim SL, Kim EM, Kim DW, Lim ST, Jang KY, Jeong YY, Nah JW, Sohn MH: **SPION-loaded chitosan-linoleic acid nanoparticles to target hepatocytes.** *Int J Pharm* 2009, **371:**163–169.
67. Huang Y, Yu H, Guo L, Huang Q: **Structure and self-assembly properties of a new chitosan-based amphiphile.** *J Phys Chem B* 2010, **114:**7719–7726.
68. Sajomsang W, Tantayanon S, Tangpasuthadol V, Thatte M, Daly WH: **Synthesis and characterization of N-aryl chitosan derivatives.** *Int J Biol Macromol* 2008, **43:**79–87.
69. Yang Q, Shuai L, Pan X: **Synthesis of fluorescent chitosan and its application in noncovalent functionalization of carbon nanotubes.** *Biomacromolecules* 2008, **9:**3422–3426.
70. Park JH, Saravanakumar G, Kim K, Kwon IC: **Targeted delivery of low molecular drugs using chitosan and its derivatives.** *Adv Drug Deliv Rev* 2010, **62:**28–41.
71. Lee SJ, Park K, Oh YK, Kwon SH, Her S, Kim IS, Choi K, Lee SJ, Kim H, Lee SG, Kim K, Kwon IC: **Tumor specificity and therapeutic efficacy of photosensitizer-encapsulated glycol chitosan-based nanoparticles in tumor-bearing mice.** *Biomaterials* 2009, **30:**2929–2939.
72. Hwang HY, Kim IS, Kwon IC, Kim YH: **Tumor targetability and antitumor effect of docetaxel-loaded hydrophobically modified glycol chitosan nanoparticles.** *J Control Release* 2008, **128:**23–31.
73. Lim EK, Yang J, Dinney CP, Suh JS, Huh YM, Haam S: **Self-assembled fluorescent magnetic nanoprobes for multimode-biomedical imaging.** *Biomaterials* 2010, **31:**9310–9319.
74. Lim EK, Kim HO, Jang E, Park J, Lee K, Suh JS, Huh YM, Haam S: **Hyaluronan-modified magnetic nanoclusters for detection of CD44-overexpressing breast cancer by MR imaging.** *Biomaterials* 2011, **32:**7941–7950.
75. Yang J, Lim EK, Lee HJ, Park J, Lee SC, Lee K, Yoon HG, Suh JS, Huh YM, Haam S: **Fluorescent magnetic nanohybrids as multimodal imaging agents for human epithelial cancer detection.** *Biomaterials* 2008, **29:**2548–2555.
76. Lee T, Lim EK, Lee J, Kang B, Choi J, Park HS, Suh JS, Huh YM, Haam S: **Efficient CD44-targeted magnetic resonance imaging (MRI) of breast cancer cells using hyaluronic acid (HA)-modified MnFe2O4 nanocrystals.** *Nanoscale Res Lett* 2013, **8:**149.
77. Lim E-K, Jang E, Kim B, Choi J, Lee K, Suh J-S, Huh Y-M, Haam S: **Dextran-coated magnetic nanoclusters as highly sensitive contrast agents for magnetic resonance imaging of inflammatory macrophages.** *J Mater Chem* 2011, **21:**12473.
78. Lim EK, Kim B, Choi Y, Ro Y, Cho EJ, Lee JH, Ryu SH, Suh JS, Haam S, Huh YM: **Aptamer-conjugated magnetic nanoparticles enable efficient targeted detection of integrin alphavbeta3 via magnetic resonance imaging.** *J Biomed Mater Res A* 2013. doi:10.1002/jbm.a.34678.
79. Li M, Hong Y, Wang Z, Chen S, Gao M, Kwok RT, Qin W, Lam JW, Zheng Q, Tang BZ: **Fabrication of chitosan nanoparticles with aggregation-induced emission characteristics and their applications in long-term live cell imaging.** *Macromol Rapid Commun* 2013, **34:**767–771.
80. Kamada H, Tsutsumi Y, Sato-Kamada K, Yamamoto Y, Yoshioka Y, Okamoto T, Nakagawa S, Nagata S, Mayumi T: **Synthesis of a poly(vinylpyrrolidone-co-dimethyl maleic anhydride) co-polymer and its application for renal drug targeting.** *Nat Biotechnol* 2003, **21:**399–404.

81. Meyer M, Zintchenko A, Ogris M, Wagner E: **A dimethylmaleic acid-melittin-polylysine conjugate with reduced toxicity, pH-triggered endosomolytic activity and enhanced gene transfer potential.** *J Gene Med* 2007, **9:**797–805.
82. Yao K, Chen Y, Zhang J, Bunyard C, Tang C: **Cationic salt-responsive bottle-brush polymers.** *Macromol Rapid Commun* 2013, **34:**645–651.
83. Shanta Singh N, Kulkarni H, Pradhan L, Bahadur D: **A multifunctional biphasic suspension of mesoporous silica encapsulated with YVO4:Eu3+ and Fe3O4 nanoparticles: synergistic effect towards cancer therapy and imaging.** *Nanotechnology* 2013, **24:**065101.
84. Venkataraman S, Chowdhury ZA, Lee AL, Tong YW, Akiba I, Yang YY: **Access to different nanostructures via self-assembly of thiourea-containing PEGylated amphiphiles.** *Macromol Rapid Commun* 2013, **34:**652–658.
85. MacNeill CM, Coffin RC, Carroll DL, Levi-Polyachenko NH: **Low band gap donor-acceptor conjugated polymer nanoparticles and their NIR-mediated thermal ablation of cancer cells.** *Macromol Biosci* 2013, **13:**28–34.
86. Banerjee S, Sen K, Pal TK, Guha SK: **Poly(styrene-co-maleic acid)-based pH-sensitive liposomes mediate cytosolic delivery of drugs for enhanced cancer chemotherapy.** *Int J Pharm* 2012, **436:**786–797.
87. Huang C, Tang Z, Zhou Y, Zhou X, Jin Y, Li D, Yang Y, Zhou S: **Magnetic micelles as a potential platform for dual targeted drug delivery in cancer therapy.** *Int J Pharm* 2012, **429:**113–122.
88. Li S, Su Z, Sun M, Xiao Y, Cao F, Huang A, Li H, Ping Q, Zhang C: **An arginine derivative contained nanostructure lipid carriers with pH-sensitive membranolytic capability for lysosomolytic anti-cancer drug delivery.** *Int J Pharm* 2012, **436:**248–257.
89. Ding Y, Wang W, Feng M, Wang Y, Zhou J, Ding X, Zhou X, Liu C, Wang R, Zhang Q: **A biomimetic nanovector-mediated targeted cholesterol-conjugated siRNA delivery for tumor gene therapy.** *Biomaterials* 2012, **33:**8893–8905.

doi:10.1186/1556-276X-8-467
Cite this article as: Lim *et al.*: Chitosan-based intelligent theragnosis nanocomposites enable pH-sensitive drug release with MR-guided imaging for cancer therapy. *Nanoscale Research Letters* 2013 **8**:467.